CHARACTERISTICS OF PARAMETER UNCERTAINTY OF THE EMBRACE METHOD BASED ON MONTE CARLO SIMULATIONS

Yochan Kim[1], Jaewhan Kim[1]

[1] *Risk Assessment Research Division, Korea Atomic Energy Research Institute, Yuseong-gu, Daejeon 34057, Republic of Korea, yochankim@kaeri.re.kr*

ABSTRACT

Characterizing and understanding the uncertainties of human reliability is a critical aspect of the risk-related decision-making process. Among various kinds of uncertainties, parametric uncertainty of human error probability (HEP) reflects variabilities in the method-dependent parameters, such as nominal HEP, effects of performance shaping factors on HEPs, and recovery factors. Because of a lack of data supporting these kinds of parametric bounds, the rules for bound determination in human reliability analysis (HRA) methods have not been grounded on sufficient evidence. This study attempts to estimate uncertainty bounds for parametric uncertainty using Monte Carlo simulations. Extending the authors' study, here uncertainties residing in the error rates of local manipulations and recovery behaviors were additionally involved in the simulations. Based on the results of this empirical estimation, we derived the characteristics of parametric uncertainties based on the failures and elements with the highest contribution. We expect that these characteristics will be useful in understanding the uncertainty of human reliability.

Keywords: Human error probability, Human reliability analysis, Monte Carlo simulation, Parameter uncertainty, Uncertainty analysis

I. INTRODUCTION

Human reliability analysis (HRA) is a key part of probabilistic safety assessment (PSA) that looks at how people interact with systems during specific events, examines how these interactions can fail, and calculates the chance of human errors occurring (known as human error probability or HEP) in these events [1]. However, in order to facilitate the application of HRA, HRA models simply represent the complex processes of human–system interactions and cognitive behaviors and rely on estimates from expert opinions or data extracted from similar contexts due to insufficient empirical data [2]. Therefore, a clear understanding and utilization of the uncertainty in HRA is necessary for risk-based decision making. Many uncertainty guidelines generally classify uncertainties into three categories: parameter, model, and completeness [3,4]. Among them, parameter uncertainty is associated with the values of the component parameters in the HRA model, such as the nominal HEPs, performance shaping factor (PSF) multipliers, and recovery multipliers. Current HRA methods employ beta or lognormal distributions to anticipate the parameter bounds [2]. In the case of lognormal distributions, the error factor, which is the ratio between the median and the 5th percentile or between the median and the 95th percentile, is often calculated to represent the bounds. When a random variable X is lognormally distributed, $\ln(X) \sim N(mu, sigma^2)$, *sigma* is equivalent with ln(error factor)/1.645.

The authors' previous study attempted to estimate the bounds of HEP values that an HRA method can inherently produce [2]. To this end, we categorized the component parameters into method-dependent parameters and scenario-specific parameters and conducted random sampling according to the distribution of the method-dependent parameters within several scenario-specific parameter values found during current application examples of HRA. As a result, we showed that the HEP variable most closely matches the lognormal distribution and suggested that the error factor value according to the range of HEP can be used as a rule for estimating the parameter uncertainty of HEP. However, the paper also alluded to the fact that parameter uncertainties can be determined by factors other than simply the HEP magnitude. Therefore, the present study revisits the simulation data for understanding the root causes of the uncertainty variabilities of the EMBRACE (Empirical Data-Based Crew Reliability Assessment and Cognitive Error Analysis) method, following previous studies. Prior to this, in order to overcome the limitations of the previous Monte Carlo simulation, the simulation data are regenerated by (1) adding component parameters regarding local operation and (2) considering the uncertainty in recovery multipliers. We then compare the statistical models that best explain the samples generated by Monte Carlo simulation using statistical measures and discuss the causes that explain the dispersion of the samples, focusing on the failure probabilities and the component parameters.

II. UNCERTAINTY PROPAGATION OF EMBRACE PARAMETERS

II.A. Monte Carlo Analysis

In this study, HEP values derived from the EMBRACE method [5,6] are generated by the Monte Carlo method [7]. The EMBRACE method is based on the nominal HEPs estimated from HuREX data and the PSF multipliers elicited from a formal expert evaluation process, which provides concrete evidence for the distribution of the component parameters. The method-dependent parameters and scenario-specific parameters of the EMBRACE method can be distinguished as shown in Fig. 1.

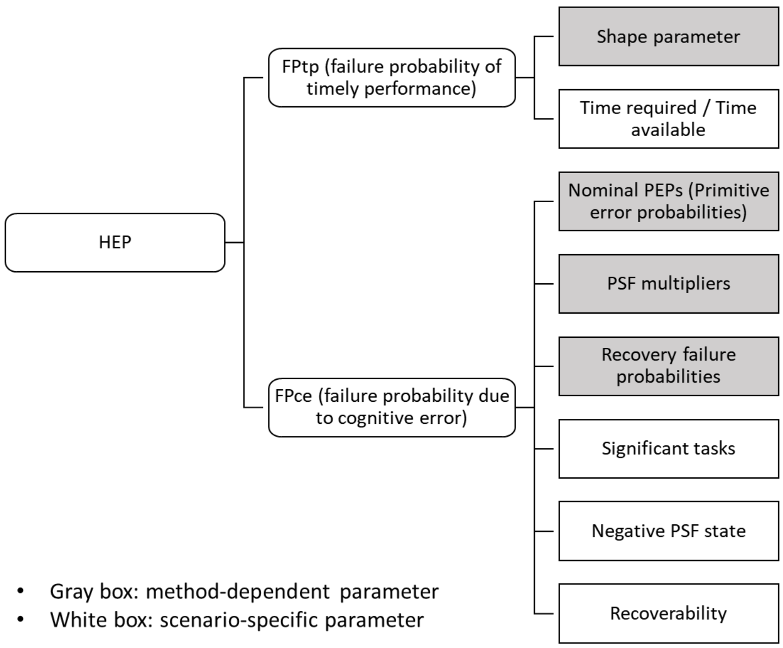

FIGURE 1. Method-dependent parameters and scenario-specific parameters of the EMBRACE method.

In the EMBRACE method, an HEP is calculated using Eqs. (1), (2), and (3):

$$HEP = FPtp + FPce\ , \tag{1}$$

where *FPtp* is the failure probability of timely performance and *FPce* is the failure probability due to cognitive error,

$$FPtp = 1 - \Phi\left[\frac{\ln(TR)}{\sigma}\right]\ , \tag{2}$$

where Φ is the cumulative probability function of the standard normal distribution, *TR* is the time required divided by the time available, and σ is the standard deviation of the log of the distribution, and

$$FPce = \prod_{L} RM_L \sum_{j}\left[\prod_{M_j} PSFM_{M_j} \sum_{N_{ij}} NPEP_{N_{ij}}\right], \tag{3}$$

where $NPEP_{Nij}$ is the *N*th type of nominal primitive error probability (PEP) for the *i*th task in the *j*th step, $PSFM_{Mj}$ is the *M*th type of PSF multiplier in the *j*th step, and RM_L is the *L*th type of recovery multiplier.

II.A.1. Scenario-Specific Parameters

The scenario-specific parameters were determined by randomly selecting examples from APR1400 application cases [6]. For instance, 28 primitive task combinations were extracted from the APR1400 procedure steps. For each HEP simulation run, one, two, or three task combinations were randomly selected. At this time, one or zero PSFs for each combination could have negative values so that PSFM could be multiplied by each combination. In addition, assuming that one, two, or three recoveries were applicable, the recovery sources to be applied were randomly selected. The TR value was then randomly selected from one of the 22 values in the time analysis cases for the APR1400. Through this process, a total of 40 scenario-specific parameter combinations were generated. Table I shows a summary of the 40 scenario-specific cases.

TABLE I. Summary of scenario-specific parameter values for Monte Carlo simulation

Scenario ID	Step number	Task number for each step	Negative PSF	Recovery attempt number	TR
1	2	(1) 11 (2) 13	(1) Independent reviewer (Execution) (2) Complexity of required task (Execution)	1	0.31
2	3	(1) 5 (2) 8 (3) 11	(1) (All positive) (2) Training level (Execution) (3) (All positive)	1	0.11
3	3	(1) 6 (2) 3 (3) 5	(1) Subjective stress (Transition) (2) Support function of computer-based procedure (Execution) (3) (All positive)	1	0.30
4	2	(1) 8 (2) 11	(1) (All positive) (2) Independent reviewer (Execution)	3	0.40
5	1	(1) 8	(1) (All positive)	0	0.30
6	3	(1) 5 (2) 7 (3) 10	(1) (All positive) (2) (All positive) (3) (All positive)	0	0.47
7	3	(1) 9 (2) 5 (3) 5	(1) Career-experience level (Transition) (2) Complexity of human–machine interface (Transition) (3) Support function of computer-based procedure (Transition)	0	0.73
8	2	(1) 3 (2) 6	(1) Complexity of required task (Transition) (2) Complexity of human–machine interface (Transition)	0	0.11
9	3	(1) 10 (2) 11 (3) 6	(1) (All positive) (2) Support function of computer-based procedure (Transition) (3) (All positive)	2	0.14
10	3	(1) 11 (2) 10 (3) 7	(1) (All positive) (2) (All positive) (3) (All positive)	0	0.31
11	1	(1) 13	(1) Career-experience level (Transition)	0	0.80
12	2	(1) 11	(1) Career-experience level (Transition) (2) Subjective stress (Transition)	0	0.30
13	2	(1) 5 (2) 6	(1) (All positive) (2) (All positive)	0	0.73
14	2	(1) 5 (2) 6	(1) (All positive) (2) Independent reviewer (Transition)	3	0.73
15	1	(1) 10	(1) Communication level (Execution)	3	0.50
16	3	(1) 8 (2) 7 (3) 10	(1) Procedure quality (Execution) (2) (All positive) (3) (All positive)	3	0.10

17	3	(1) 8 (2) 3 (3) 10	(1) Procedure quality (Transition) (2) Procedure quality (Execution) (3) Independent reviewer (Transition)	3	0.11
18	2	(1) 6 (2) 5	(1) (All positive) (2) Crew dynamics (Transition)	3	0.40
19	2	(1) 12 (2) 6	(1) Subjective stress (Transition) (2) Training level (Transition)	2	0.08
20	1	(1) 9	(1) (All positive)	1	0.30
21	1	(1) 9	(1) (All positive)	3	1.00
22	2	(1) 5 (2) 6	(1) Career-experience level (Transition) (2) (All positive)	2	0.08
23	3	(1) 10 (2) 6 (3) 5	(1) (All positive) (2) Complexity of human–machine interface (Transition) (3) (All positive)	1	0.77
24	3	(1) 9 (2) 7 (3) 12	(1) Career-experience level (Execution) (2) (All positive) (3) (All positive)	2	0.35
25	2	(1) 9 (2) 11	(1) (All positive) (2) (All positive)	3	0.30
26	3	(1) 5 (2) 10 (3) 12	(1) Career-experience level (Execution) (2) Training level (Execution) (3) (All positive)	1	0.80
27	2	(1) 7 (2) 5	(1) (All positive) (2) (All positive)	0	0.23
28	1	(1) 3	(1) (All positive)	0	0.18
29	3	(1) 6 (2) 7 (3) 12	(1) Career-experience level (Execution) (2) (All positive) (3) (All positive)	0	0.73
30	3	(1) 5 (2) 7 (3) 5	(1) (All positive) (2) (All positive) (3) Procedure quality (Execution)	2	0.10
31	1	(1) 9	(1) (All positive)	3	0.40
32	3	(1) 5 (2) 6 (3) 9	(1) (All positive) (2) Procedure quality (Transition) (3) Communication level (Transition)	3	0.13
33	1	(1) 12	(1) Subjective stress (Execution)	0	0.13
34	2	(1) 7 (2) 3	(1) Training level (Transition) (2) Independent reviewer (Execution)	1	0.50
35	3	(1) 11 (2) 9 (3) 5	(1) Communication level (Transition) (2) Communication level (Transition) (3) Training level (Execution)	1	0.03
36	2	(1) 7 (2) 5	(1) (All positive) (2) (All positive)	2	0.18
37	1	(1) 5	(1) Training level (Transition)	0	0.47
38	2	(1) 5 (2) 11	(1) (All positive) 2) Procedure quality (Transition)	1	0.77
39	2	(1) 5 (2) 10	(1) Complexity of human–machine interface (Transition) (2) Career-experience level (Transition)	0	0.77
40	2	(1) 7 (2) 3	(1) (All positive) (2) (All positive)	3	0.50

II.A.2. Method-Dependent Parameters

Table II shows the median, 5th percentile, and 95th percentile of four types of method-dependent parameters. Most parameters are known to be most closely described by the lognormal distribution [5,6,8,9,10], while in the case of the PEP for situation understanding tasks, the beta distribution was used to estimate the PEP values [6]. For the parameters following a lognormal distribution, the median value and error factor value were used to estimate the parameter. In the case of FPtp, the median value was set when the shape parameter was 0.3403, and the error factor was calculated by regarding the values when the shape parameter was 0.4248 and 0.2766 as the 95th and 5th percentiles [5]. For the parameters following a beta distribution, the alpha and beta parameters derived from Bayesian inference were employed directly. A total of 10,000 random samples were generated from the lognormal or beta distribution of each component, and HEPs were calculated by combining them with scenario-specific parameters.

TABLE II. Distribution of the method-dependent parameters

Category	Parameter name	Median	5th percentile	95th percentile	Ref.
NPEP	Detection–trend	3.08E-04	1.02E-04	9.27E-04	[6,8]
	Detection–synthesis	1.51E-03	4.71E-04	4.80E-03	[6,8]
	Detection–others	1.10E-04	4.31E-05	2.81E-04	[6,8]
	Situation understanding (Beta distribution)	2.16E-03	3.22E-04	7.09E-03	[6,8]
	Decision–sequential step entry or Decision–external communication	1.85E-04	1.01E-04	3.39E-04	[6,8]
	Decision–procedure transfer or Decision–step transfer	5.62E-03	4.13E-03	7.47E-03	[6,8]
	Decision–detection	6.22E-05	3.28E-05	1.18E-04	[6,8]
	Decision–manipulation	1.96E-03	1.12E-03	3.38E-03	[6,8]
	Execution–single discrete manipulation or Execution–external communication	1.84E-03	1.20E-03	2.79E-03	[6,8]
	Execution–single continuous manipulation	1.53E-02	6.47E-03	3.19E-02	[6,8]
	Execution–dynamic manipulation	1.49E-02	7.51E-03	2.82E-02	[6,8]
	Execution-local discrete manipulation	5.00E-03	1.00E-03	2.50E-02	[10]
	Execution-local dynamic manipulation	1.00E-02	2.00E-03	5.00E-02	[10]
PSFM for transition	Complexity of required task	3	2	10	[6,8]
	Subjective stress	5	2	10	[6,8]
	Complexity of human–machine interface	3	1	5	[6,8]
	Procedure quality	5	3	20	[6,8]
	Support function of computer-based procedure	2	1	3	[6,8]
	Independent reviewer	3	1	5	[6,8]
	Crew dynamics	1	1	2	[6,8]
	Communication level	2	1	3	[6,8]
	Training level	5	3	20	[6,8]
	Career-experience level	5	3	20	[6,8]
PSFM for execution	Complexity of required task	3	2	10	[6,8]
	Subjective stress	5	2	10	[6,8]
	Complexity of human–machine interface	5	2	20	[6,8]
	Procedure quality	5	3	20	[6,8]
	Support function of computer-based procedure	3	1	5	[6,8]
	Independent reviewer	3	1	10	[6,8]
	Crew dynamics	1	1	2	[6,8]
	Communication level	2	1	5	[6,8]
	Training level	3	2	5	[6,8]
RM	Review after shift change	0.0164	0.0082	0.0328	[10]
	Review after procedure completion	0.05	0.018	0.14	[10]
	Advisor’s monitoring–first check	0.5	0.25	1	[10]
	Advisor’s monitoring–second check	0.14	0.04	0.5	[10]

	Step reviewing result	0.5	0.25	1	[10]
FPtp	FPtp	$1 - \Phi[\ln(TR)/0.3403]$	$1 - \Phi[\ln(TR)/0.2766]$	$1 - \Phi[\ln(TR)/0.4248]$	[5]

II.B. Statistical Distribution Fitting

Table III shows the means of HEP, FPtp, and FPce calculated from 10,000 Monte Carlo samples. Among the 40 scenario cases, FPtp was calculated higher in 18 cases, and FPce was superior in the remaining 22 cases. We compared which statistical model best explained the distributions of HEP values among Weibull, normal, lognormal, exponential, and beta distributions. The results of comparing the goodness-of-fit using the Bayesian information criterion (BIC) and Akaike information criterion (AIC) measures revealed that the lognormal distribution provided models that best explained the HEPs in all cases. This is because most of the method-dependent parameters of EMBRACE follow the lognormal distribution.

TABLE III. Mean values of the simulation samples and estimates for lognormal distributions

Scenario ID	HEP mean	FPtp mean	FPce mean	*mu*	*sigma*	exp (*mu*)	Error factor
1	3.12E-02	1.36E-03	2.98E-02	−3.7969	0.807401	0.02244	3.77415
2	3.34E-03	1.00E-06	3.34E-03	−5.80472	0.45193	0.003013	2.10313
3	5.10E-03	1.04E-03	4.06E-03	−5.61288	0.796492	0.003651	3.70702
4	6.43E-03	6.43E-03	1.00E-06	−5.64835	1.09252	0.003523	6.0327
5	5.70E-03	1.13E-03	4.58E-03	−5.25482	0.34077	0.005222	1.75166
6	4.13E-02	1.72E-02	2.41E-02	−3.25275	0.346237	0.038668	1.76749
7	2.24E-01	1.84E-01	3.99E-02	−1.51491	0.189006	0.219827	1.36467
8	2.06E-02	1.00E-06	2.06E-02	−4.04016	0.557961	0.017595	2.50389
9	5.40E-05	1.00E-06	5.30E-05	−10.1841	0.84808	3.78E-05	4.03535
10	1.22E-02	1.43E-03	1.07E-02	−4.45038	0.233364	0.011674	1.46797
11	4.36E-01	2.57E-01	1.80E-01	−0.86441	0.257481	0.4213	1.52738
12	8.84E-02	1.15E-03	8.73E-02	−2.63458	0.644101	0.071749	2.88506
13	1.90E-01	1.84E-01	6.10E-03	−1.67613	0.16998	0.187097	1.32262
14	1.84E-01	1.84E-01	3.30E-05	−1.70744	0.174115	0.181329	1.33165
15	2.56E-02	2.56E-02	2.00E-06	−3.87966	0.653845	0.020658	2.93168
16	1.70E-05	1.00E-06	1.60E-05	−11.4394	0.942451	1.08E-05	4.71304
17	1.86E-03	1.00E-06	1.86E-03	−7.14578	1.306375	0.000788	8.57617
18	6.42E-03	6.30E-03	1.19E-04	−5.59127	1.038492	0.00373	5.51968
19	3.84E-04	1.00E-06	3.83E-04	−8.75841	1.324959	0.000157	8.84239
20	4.64E-03	1.11E-03	3.54E-03	−5.5471	0.528738	0.003899	2.38637
21	5.00E-01	5.00E-01	4.20E-05	−0.69306	0.000108	0.500042	1.00018
22	1.25E-03	1.00E-06	1.25E-03	−7.19002	1.001934	0.000754	5.19752
23	2.27E-01	2.26E-01	9.71E-04	−1.48954	0.13208	0.225477	1.24268
24	3.48E-03	2.80E-03	6.73E-04	−6.25344	0.988996	0.001924	5.08807
25	1.15E-03	1.15E-03	7.00E-06	−8.41806	1.74344	0.000221	17.6011
26	2.62E-01	2.57E-01	4.59E-03	−1.34527	0.108128	0.26047	1.19467
27	2.49E-02	2.43E-04	2.46E-02	−3.73083	0.26744	0.023973	1.55261
28	6.07E-03	1.60E-04	5.91E-03	−5.13759	0.189119	0.005872	1.36493
29	2.42E-01	1.84E-01	5.82E-02	−1.43336	0.173711	0.238506	1.33077
30	2.18E-03	1.00E-06	2.18E-03	−6.49762	0.861451	0.001507	4.12508
31	6.49E-03	6.48E-03	1.20E-05	−5.64347	1.089725	0.003541	6.00503
32	1.12E-04	1.00E-06	1.11E-04	−9.47932	0.869753	7.64E-05	4.18181
33	6.94E-02	1.00E-06	6.94E-02	−2.79994	0.513144	0.060814	2.32593
34	5.30E-02	2.55E-02	2.74E-02	−3.14204	0.619842	0.043194	2.7722
35	5.77E-03	1.00E-06	5.77E-03	−5.52182	0.845858	0.003999	4.02062
36	1.09E-04	8.30E-05	2.70E-05	−10.5947	1.0199	2.5E-05	5.35342
37	5.43E-02	1.68E-02	3.75E-02	−3.05301	0.522682	0.047217	2.36272
38	2.30E-01	2.27E-01	3.35E-03	−1.47787	0.131956	0.228123	1.24243

39	2.47E-01	2.26E-01	2.10E-02	−1.40508	0.130892	0.245347	1.24026
40	2.60E-02	2.59E-02	7.20E-05	−3.86554	0.657314	0.020952	2.94845

The parameters when fitting the HEP distribution to the lognormal distribution are thus shown in the fifth and sixth columns of Table III. The exponentiated *mu* shown in the seventh column indicates the median of the HEP estimated by the fitted lognormal distribution. The last column presents the error factor values according to the lognormal distribution.

III. DISCUSSION ON THE CHARACTERISTICS OF UNCERTAINTY BOUNDS

The characteristics of the parameter uncertainty bounds of HEPs can be discussed based on the relationship between exponentiated *mu* and error factor. A scatter plot of the exponentiated *mu* and error factor can be depicted as in Fig. 2. Here, the blue diamonds indicate cases where FPtp is higher than FPce, and the green triangles indicate cases where FPce is higher than FPtp. By examining Table III and Fig. 2, the uncertainty bounds of HEP can be said to have the following characteristics. First, when FPtp exceeds FPce, a typical trend of the uncertainty bounds of FPtp is observed. Table IV shows the relationship between FPtp values and their error factors presented in the previous report. Most blue diamonds in Fig. 2 are coincident with Table IV. For example, scenario ID 25 has an error factor of HEP higher than 17, which is consistent with the third row in Table IV. On the other hand, for ID 36, the error factor is not high even though the HEP is low. This can be attributed to the fact that FPce also affects the error factor because FPtp and FPce have similar values.

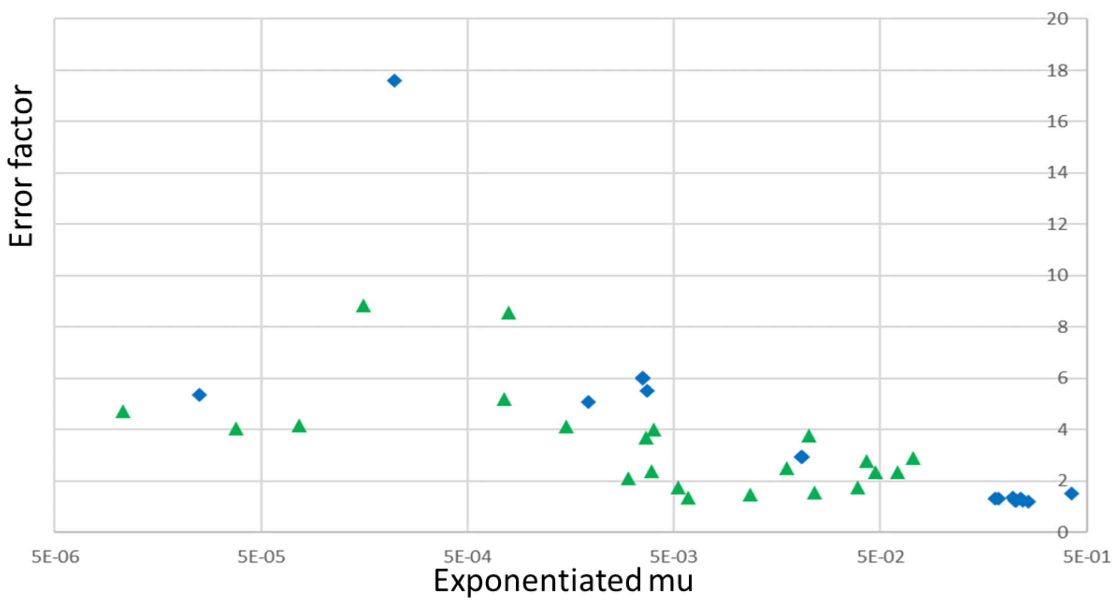

FIGURE 2. Scatter plot between exponentiated *mu* (x-axis) and error factor (y-axis).

TABLE IV. Uncertainty bound rule for FPtp in [5]

FPtp range	Error factor
0.5 <= FPtp	1
0.05 <= FPtp < 0.5	2
0.01 <= FPtp < 0.05	3
0.006 <= FPtp < 0.01	4
0.003 <= FPtp < 0.006	5
0.001 <= FPtp < 0.003	7.5
1.0E-4 <= FPtp < 0.001	17
1.0E-5 <= FPtp < 1.0E-4	40
FPtp < 1.0E-5	90

Second, when FPce is superior to FPtp, the error factor is found to have a value between 2 and 10. It is observed that the magnitude of the error factor is influenced not only by the dimensions of the HEP or FPce but also by the quantity of primitive tasks evaluated, the PSF multipliers applied, or the recovery multipliers considered. When the number of primitive tasks, the number of negative PSF states, and the number of recovery factors are noted as a, b, and c, respectively, $a*(b+1)*(c+1)-2$ could be a measure for the number of the component variables included (note that this scale adds 1 to b and c to avoid cases where the formula produces 0 when b and c are 0). Figure 3 shows the correlation between the variable number measure and the magnitude of the error factor. In general, it is understood that as the number of component variables increases or the HEP diminishes, the error factor escalates.

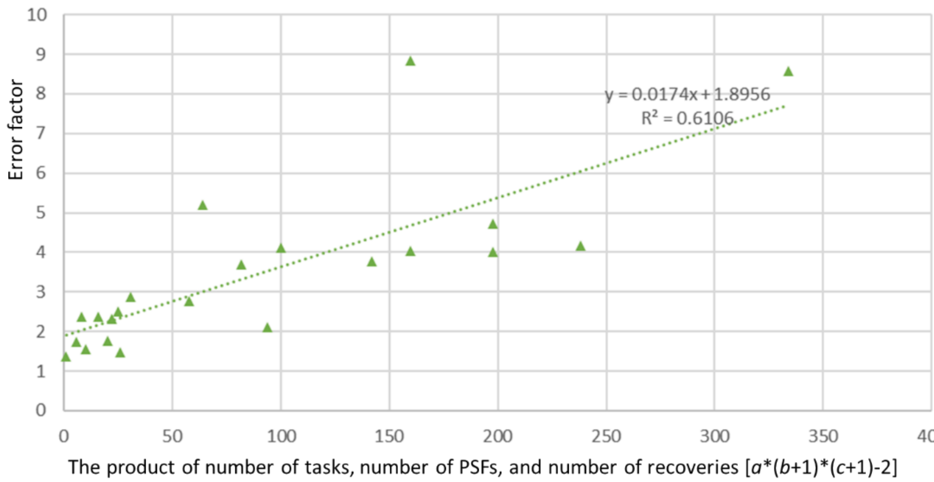

FIGURE 3. Scatter plot between the product of number of tasks included, number of PSFs having a negative state, and number of recoveries applied (x-axis), and error factor (y-axis).

Considering the trend of the error factor presented in Fig. 2, it is interpreted that the error factor determination rule according to the HEP range proposed in [2] (refer to Table V) conservatively explains the parameter uncertainty bound of HEP overall. However, it is difficult to estimate the parameter uncertainty of HEPs smaller than 1.0E-03. In particular, additional research is needed regarding the fact that an FPtp lower than 1.E-03 has a high error factor.

In addition, this study suggests that the determination rule in Table V can be modified to predict the uncertainty bounds more accurately. Since the trend of error factors varies slightly depending on whether FPtp or FPce is more dominant within HEP, different rules can be applied depending on their dominance. For example, the error factor of FPce can be anticipated based on the FPce range, as seen in Table VI. Therefore, after identifying the factor that has a greater impact on HEP between FPtp and FPce, HRA practitioners can employ either Table IV or VI as the rule for determining the error factor.

TABLE V. Uncertainty bound rule for HEP proposed in [2]

HEP range	Error factor
0.5 <= HEP	1
0.03 <= HEP < 0.5	3
0.01 <= HEP < 0.03	4
0.006 <= HEP < 0.01	5
0.001 <= HEP < 0.006	7
HEP < 0.001	10

TABLE VI. Uncertainty bound rule for FPce proposed based on Fig. 2

FPce range	Error factor
0.5 <= FPce	1
0.07 <= FPce < 0.5	2
0.03 <= FPce < 0.07	3
0.001 <= FPce < 0.03	4
FPce < 0.001	10

IV. CONCLUSION AND FUTURE WORKS

This study extended the Monte Carlo analysis developed in [2] to generate samples additionally considering the distributions of component parameters related to local manipulations and recovery behaviors and discussed parameter uncertainty rules that can apply to the results of HRA. Since many component parameters are mostly represented by lognormal distributions [2,5,6,11], it seems statistically appropriate to interpret HEP uncertainties with lognormal models. Therefore, the results of this paper reverified that the determination rule proposed in [2] conservatively describes the distribution of error factors with the assumption that simulated HEPs follow lognormal distributions. That is, it is judged that the results of Table V provide a reasonable approximation according to the parameter uncertainty rule of the EMBRACE method. For a more precise estimation, combining Table IV and Table VI can be a beneficial alternative by identifying which factor more significantly contributes to HEP among FPtp and FPce. These suggestions are believed to be realistic and pragmatic because a lot of human performance times are described with lognormal distributions [11] and because HEPs in existing PSA models are often assumed to be lognormally distributed with their uncertainties expressed using error factors. However, it should also be noted that HRA methods can have different distributions for uncertainty assessments depending on the purpose of the HRA application or the combination with a PSA model. In addition, more evidence should be generated to gain a clearer understanding of parameter uncertainty calculations through additional data collection and collaboration with HRA/PSA practitioners.

It is noted that this study used exponentiated *mu* to scrutinize the tendency of the error factor. The exponentiated *mu* implies the median value of HEP, which may differ from the mean value. In particular, low HEP values are expected to have a large difference between the median and the mean. We believe that additional research is needed on the accuracy of parameter uncertainty estimation in such cases.

ACKNOWLEDGMENTS

This work was supported by the Nuclear Safety Research Program through the Korea Foundation of Nuclear Safety (KoFONS) using a financial resource granted by the Nuclear Safety and Security Commission (NSSC) of the Republic of Korea (No. 2106054).

REFERENCES

[1] R. L. BORING, “Fifty years of THERP and human reliability analysis,” *INL report*, No. INL/CON-12-25623. Idaho National Lab.(INL), Idaho Falls, ID (United States), (2012).
[2] Y. KIM, J. KIM, and D. S. KIM, "Estimating parameter uncertainty bounds of human error probability using Monte Carlo simulation," *Annals of Nuclear Energy*, 211, 111024, (2025).
[3] EPRI, “Practical guidance on the use of probabilistic risk assessment in risk-informed applications with a focus on the treatment of uncertainty”, *EPRI report*, 1026511, (2012).
[4] US NRC, “Guidance on the Treatment of Uncertainties Associated With PRAs in Risk-Informed Decisionmaking,” *NUREG-1855, Revision 1*. Office of Nuclear Regulatory Research, US Nuclear Regulatory Commission (2017).
[5] Y. KIM, J. KIM, J. PARK, S. Y. CHOI, S. KIM, W. JUNG, H.E. KIM, & S. K. SHIN, “An HRA Method for Digital Main Control Rooms—Part I: Estimating the Failure Probability of Timely Performance,” *KAERI technical report*, KAERI/TR-7607/2019, (2019).
[6] Y. KIM, J. KIM, J. PARK, S. Y. CHOI, & S. H. KIM, “An HRA Method for Digital Main Control Rooms-Part II: Estimating the Failure Probability Due to Cognitive Error,” *KAERI technical report*, KAERI/TR-8065/2020, (2020).
[7] E. Zio, *Monte carlo simulation: The method." The Monte Carlo simulation method for system reliability and risk analysis.* London: Springer London, (2012).
[8] Y. KIM, “Estimate Comparison of Human Reliability Regression Models in Differently Classified Human Errors,” *ASRAM2022 (Asian Symposium on Risk Assessment and Management 2022)*, November, Daejeon, Korea, (2022).
[9] Y. KIM, “Expert elicitation for estimating PSF effects on HEPs in computer-based control rooms,” *29th European Safety and Reliability Conference.(ESREL 2019)* (2019).
[10] A.D. Swain and H.E. Guttmann, “Handbook of human-reliability analysis with emphasis on nuclear power plant applications,” *NUREG/CR-1278; SAND-80-0200*, Sandia National Lab. (SNL-NM), Albuquerque, NM (United States) (1983).
[11] Y. KIM and W. S. KIM. "Which distribution best describes human performance time." *In Transactions of the Korean Nuclear Society Autumn Meeting*. (2023).